A New Front-End for the LEP Injector Linac

Jean-Claude Godot, Louis Rinolfi - CERN, Geneva, Switzerland
Andrea Pisent - INFN, Legnaro, Italy
Hans Braun - PSI, Villigen, Switzerland

Abstract

For improved reliability, the front-end of the LEP Injector Linac (LIL) has been replaced. The new system has been used for LEP runs, since March'91.

The experimental results presented here show a significant improvement of beam characteristics. These results also agree well with those of the simulation programs.

I. INTRODUCTION

The LIL performance figures [1] have been found to be a factor 3 above their required values for LEP physics. In order to ensure that these good performance figures are consistently obtained, a new front-end with improved reliability and which allows easier maintenance was installed. It is composed of a thermionic gun, a bunching system and a matching section to the linac. The modulator of the thermionic gun was re-designed to provide beam pulses variable in length and current from 10 to 50 ns and 0 to 15 A respectively. The beam characteristics from the gun were simulated using the EGUN code. The simulations and the optimizations of the bunching parameters were carried out using the PARMELA program. Finally, the matching section was designed with TRANSPORT. This code was also applied to the linac in order to optimize the primary beam onto the target according to the simulation results of the new front-end. A complete description is given in [2].

II. BUNCHING REQUIREMENTS FOR POSITRON PRODUCTION

The Electron Positron Accumulator (EPA), that immediately follows LIL, has an energy acceptance of $\Delta E/E = \pm 1\%$. The energy spread in the positron bunch at the end of LIL is determined by three factors: the accepted momentum spread from the production target, the microbunch length and the beam loading. The last effect can be neglected because of the low charge. The acceptance of the magnetic channel after the converter is $\Delta E = \pm 2$ MeV [3], leading to:

$$(\Delta E/E)_{converter} = \pm 0.4\%$$

at the injection into EPA.

The contribution to energy spread resulting from the microbunch length depends directly on the bunching quality. Assuming a bunch of relativistic positrons travelling on the crest of a wave, one can calculate:

$$(\Delta E / E)_{\phi} = 1 - \cos\frac{\Delta\phi}{2} \qquad (1)$$

where $\Delta\phi = \omega\Delta t$ is the phase extension of the microbunch. If a phase extension of $\pm 8°$ from the bunching system is assumed, then $(\Delta E/E)_{\phi} = \pm 0.5\%$. The total energy spread, calculated using:

$$(\Delta E / E) = \sqrt{(\Delta E / E)^2_{\phi} + (\Delta E / E)^2_{converter}} \qquad (2)$$

is $\pm 0.64\%$, which is well within the EPA acceptance. The number of e^- in 16° of RF phase extension was chosen as the figure of merit to evaluate the performance of the bunching system.

It is interesting to observe that the energy spectrum of the primary beam is determined by the beam loading due to the high charge needed at the converter. This does not affect the $(\Delta E/E)_{\phi}$ of the positron beam as it depends only on the microbunch length. The number of e^+ and their energy spread are, by virtue of equation (1), the best test of the bunching system efficiency.

III. BEAM DYNAMICS

Fig. 1 shows a schematic layout of the new front-end. Both the pre-buncher (PB) and the buncher work at 2.99855 GHz. The first resonator is a pill-box and the second a 2/3 π standing wave structure [4]. The gun voltage is 80 kV, and the buncher provides an additional acceleration of about 4 MeV.

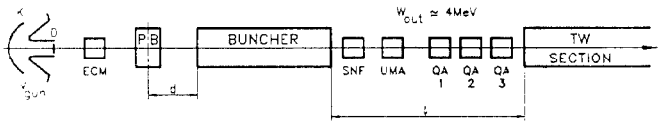

Fig. 1: Layout of the front-end

In Fig. 2, the kinetic energy of the reference particle at the end of the buncher (W_{out}) is plotted as a function of the phase ϕ_{in}; the final phase ϕ_{out} is also plotted. In the definition of these phases, there is an arbitrary offset chosen in such a way that the reference particle leaves the gun with phase equal to zero.

The two distances indicated in Fig. 1 as d and ℓ are of great importance to the longitudinal dynamics.

d is used in the pre-bunching process. The monoenergetic beam from the cathode is modulated in energy by the pre-buncher. The charge density around the reference particle is maximum after a drift space d such that:

$$\frac{d}{\lambda_{RF}} \frac{2\pi\Delta\beta}{\beta^2} \approx 1 \qquad (3)$$

where $\Delta\beta$ is the velocity modulation amplitude. In the case of low space charge, a rather long d and a low energy modula-

0-7803-0135-8/91$01.00 ©IEEE

tion is preferred. In the case of positron production the high charge in the microbunch counteracts the bunching. A short distance and a high modulation has then to be chosen. The optimum values obtained from simulations, for a beam current of 3 A, are d = 100 mm and V_{PB} = 47.1 kV, corresponding to an average accelerating field of 1.3 MV/m.

The distance ℓ is used to improve the bunching quality after the buncher. It can be seen from Fig. 2 that the reference particle at ϕ_{ref} will correspond to a minimum of the final phase and energy curves. This e^- is at the head of the bunch (with an energy of 3.8 MeV) and it is possible to bring an e^- of 4.2 MeV from the tail of the bunch to the same phase. Since $\Delta\beta/\beta$ = 0.12%, the motion is not yet completely relativistic and after 3.5 m a bunch of 20° RF is compressed to 5° RF. This is valid to a first approximation, where space charge, energy modulation before the buncher and the non-linearity of the energy modulation were neglected. According to multi-particle simulations, the bunch of 20° rotates in phase space and has a final extension of 16°.

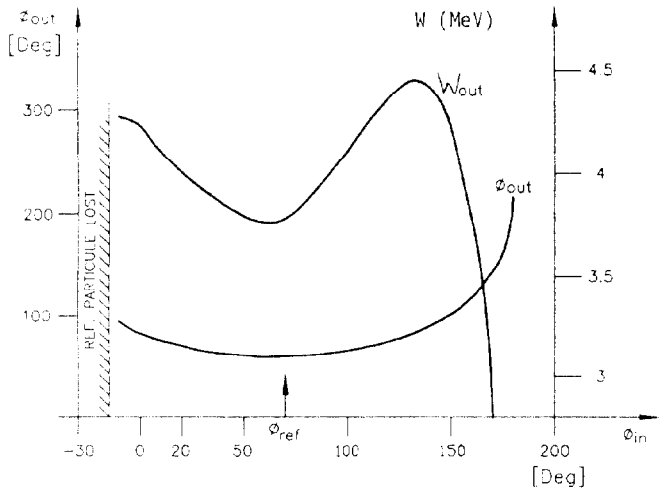

Fig. 2: Phase and kinetic energy of a single particle at buncher output versus input phase

With regard to the transverse beam dynamics, the 80 keV transport between gun and buncher is particularly delicate because of the space charge. Furthermore the surface of the cathode is spherical and the emitted current controlled by a grid, so that the emittance from the gun is of the order of 100 π mm.mrad. These problems are overcome by using a solenoidal guiding field well above the Brillouin value corresponding to 3 A of beam current. After the buncher the space charge effects become unimportant. The solenoid SNF and the triplet QA1,2,3 are used to match the beam to the first LIL accelerating section. With respect to the old front-end, the number of free parameters has been increased, so that the spot size at the converter is reduced to 1 mm (FWHH) and the maximum of the transported charge almost doubled.

Extensive calculations were performed using the three codes already mentioned. In particular for the PARMELA runs a nominal current of 3 A was chosen. Good transmission and bunching quality were found up to 9 A. Fig. 3 shows the microbunch distribution in the longitudinal phase space at the end of the matching section.

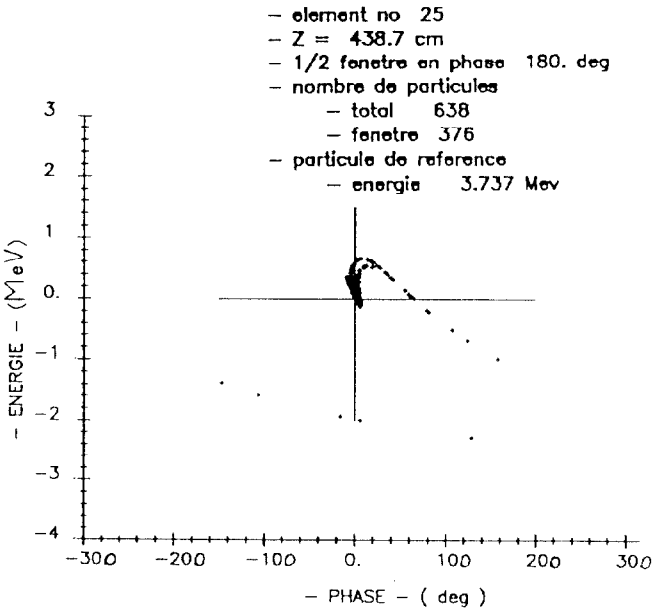

Fig. 3: Longitudinal phase space from PARMELA simulations

IV. MECHANICAL DESIGN

One of the aims of the project was to simplify mechanical design in order to have easy maintenance. This aim had to be achieved while at the same time fulfilling the quite demanding constraints imposed by the beam dynamics.

Firstly, due to the space charge effects, the distance between gun and pre-buncher has to be as short as possible.

Secondly, a standard vacuum valve is required between the gun and the pre-buncher. This valve protects the vacuum in the front-end, should the gun need to be removed, and it may also be used as a beam stopper in the safety chain.

As discussed above, the beam dynamics asks for a distance d = 100mm. To obtain this value, one side of the buncher was cut as short as possible and special bellows were welded on the pre-buncher. Finally, the buncher was mounted inside a solenoid in such a way to guarantee good continuity in the magnetic field. A spare bunching system will be realized according to this new design.

V. EXPERIMENTAL RESULTS

In order to evaluate the performance of the new front-end, the following parameters were measured. The transmission efficiencies of the bunching system and of the linac that provides the primary beam, were both measured at low and high charge values. The "non-load energy" and relative spread were measured just upstream of the target in a spectrometer line. The beam sizes were measured at the target. Finally, the yield was measured under various conditions reported in Table 1.

As already discussed in section 2, the yield measurements are, for the moment, the only data which provide a figure of merit of our bunching system. A 3 GHz RF deflector has been

installed at the buncher output, and a Tcherenkov light detector will be installed upstream of the target. This will provide a direct measure of the microbunch lengths inside the 20 ns pulse of the primary beam.

Fig. 4 displays the number of e^+ (full line) measured at the end of the linac versus the electric field in the pre-buncher.

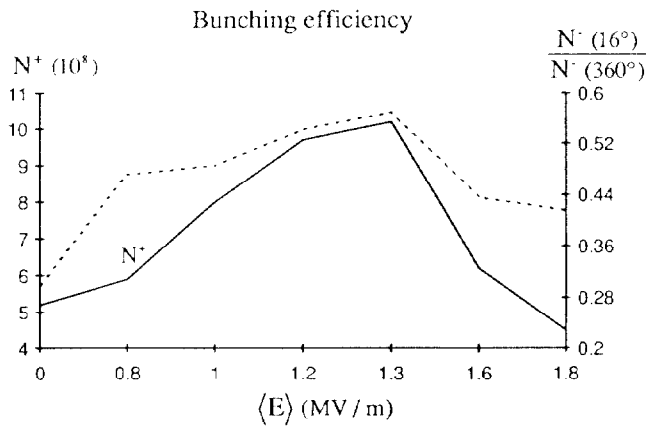

Fig. 4: Number of e^+ as a function of PB electric field

The curve is compared to the ratio N^- (16°) / N^- (360°) at the buncher output (dotted line) versus the same electric field.

The dotted line curve is obtained from PARMELA simulations and defines the bunching efficiency. The experimental and theoretical curves have their maximum at the same electric field value.

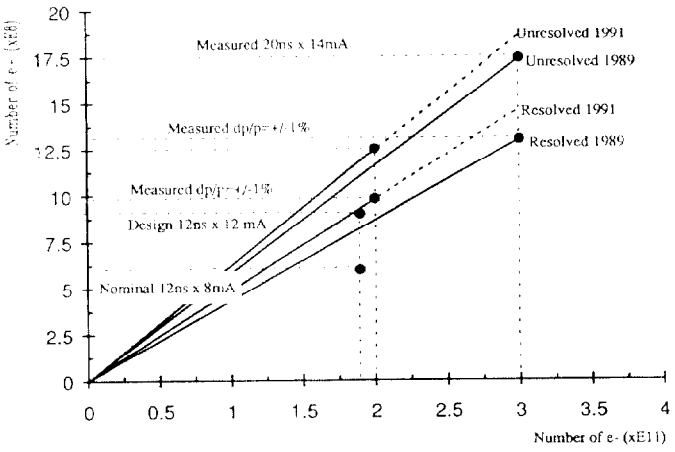

Fig. 5: LIL performance for e^+ production

The final outcome was improved reliability and increased performance figures as indicated in Fig. 5. The peak performance obtained with the old front-end [5] is compared with one experimental value obtained with the new one. The broken line is an extrapolation of expected performance with a higher primary beam charge.

Table 1: Comparison of performance

		LIL Front-End	
		1991 (New)	1989 (Peak Performance)
Gun energy	keV	80	70
Buncher output energy	MeV	4	28
No-load energy at the target	MeV	204	228
ΔE/E (full width at the base)	%	±6.6	±8
Transmission efficiency:			
- Bunching system 50 nC	%	67	66
- Bunching system 30 nC	%	72	61
- Bunching system 2 nC	%	77	56
- LIL primary beam 50 nC	%	75	76
- LIL primary beam 30 nC	%	83	83
- LIL primary beam 2 nC	%	90	90
Maximum charge at the target (e^-)	nC	83	48
For figures below, charge = 32 nC			
Beam sizes at FWHH			
- Horizontal	mm	1.0	1.0
- Vertical	mm	1.0	2.5
Unresolved yield (e^+ / e^-)	10^{-3}	6.4	5.7
Resolved yield $\frac{(e^+)}{(e^-)}$, for $\frac{\Delta E}{E} = \pm 1\%$	10^{-3}	4.9	4.3
Normalized yield $\frac{(e^+)}{(e^- \times GeV)}$, for $\frac{\Delta E}{E} = \pm 1\%$	10^{-2}	2.40	1.95

VI. CONCLUSIONS

For the LIL consolidation project, a new version of the front-end was installed. Extensive simulations based on PARMELA code allowed to find an optimized configuration. The experimental and simulation results agree to within a few per cent. With respect to LIL performance, the new front-end has given a 23% higher normalized yield. The number of positrons actually produced has been increased by 14%. Both figures have been obtained for a primary beam charge of 32 nC.

VII. REFERENCES

[1] R. Bossart, J.P. Delahaye, J.C. Godot, J.H.B. Madsen, P. Pearce, A. Riche, L. Rinolfi, "The LEP Injector Linac", CERN/PS/90-56 (LP)

[2] A. Pisent, L. Rinolfi, "A New Bunching System for the LEP Injector Linac"CERN/PS/90-58 (LP)

[3] K. Hübner, "Positron Production for Particle Accelerators", CERN/PS/88-19 (LP)

[4] A. Bensussan, D.T. Tran, D. Tronc "High Power Standing-Wave Triperiodic structure for positron acceleration", NIM 118 (1974) 349-355.

[5] J.-P. Potier, L. Rinolfi, "LPI Peak Performance recorded in December 1989", CERN Internal Note PS/LP 90-12